



J. Serb. Chem. Soc. 90 (4) 513–527 (2025)
JSCS–5403

Enhanced adsorption properties of Algerian bentonite modified by starch and glycerol for methylene blue and methyl red retention

FATIMA ZAHRA BENCHACHEM^{1,2*}, HANANE MAHROUG^{2,3}, MERIEM BENDJELLOUL⁴, ABDELKADER MIRAOU^{1,2}, EL HADJ ELANDALOUSSI⁴, KHALIL OUKEBDANE² and RANIA HALFAOUI⁵

¹Department of Industrial Engineering, Faculty of Technology, University of Tlemcen, Tlemcen, Algeria, ²Laboratory of Separation and Purification Technologies, Department of Chemistry, Faculty of Sciences, University of Tlemcen, Tlemcen, Algeria, ³Department of Hydraulic, Institute of Sciences and Technology, University center of Maghnia, Algeria, ⁴Environment and Sustainable Development Laboratory, Department of Chemistry, Faculty of Sciences and Technology, University of Relizane, Algeria and ⁵Department of Chemistry, Faculty of Sciences, University of Tlemcen, Tlemcen, Algeria

(Received 29 February, revised 22 April, accepted 24 November 2024)

Abstract: This paper describes the preparation of novel bentonite-starch composites and assesses their effectiveness as adsorbents for removing methylene blue (MB) and methyl red (MR) dyes from aqueous solutions. The adsorbents were characterized using X-ray diffraction and FTIR spectroscopy. This study is aimed to optimize the removal process by investigating the effect of pH, adsorbent dose, contact time and initial concentration. The sorption kinetics of MB and MR dyes were analysed using the pseudo-first order and pseudo-second order models. The experimental results indicate that the pseudo-second order kinetic model provides the best fit. The composite adsorbents exhibited a sorption capacity for MB, ranging from 146.21 to 157.58 mg g⁻¹ for bentonite–starch (Bt@star) and bentonite–starch–glycerol (Bt@star@gly), respectively. The sorption capacity for MR dye was 426.38 mg g⁻¹ for Bt@star and 309.82 mg g⁻¹ for Bt@star@gly. Furthermore, the correlation coefficient values indicate that the adsorption of MB and MR by Bt@star@gly is best described by the Langmuir model, which unequivocally implies that the adsorbent surface is homogeneous, resulting in monolayer adsorption. The Langmuir model also accurately describes the adsorption of MB onto Bt@Star. However, the Freundlich isotherm model is the best fit for the adsorption of MR, indicating the existence of multilayer adsorption. Finally, this study demonstrates that the composite adsorbents prepared herewith exhibit excellent adsorption performance and can be a cost-effective alternative for treating coloured wastewater.

* Corresponding author. E-mail: f.benchachem@yahoo.com
<https://doi.org/10.2298/JSC240219108B>



Keywords: composite; dyes; wastewater; kinetics.

INTRODUCTION

Organic dyes are synthetic compounds extensively used in industries of textiles, paper and plastics.¹ However, their stability and resistance to degradation make them persistent environmental pollutants.² When discharged into water bodies, these dyes can cause severe water pollution, affecting aquatic life and potentially entering the human food chain.³ The effective removal of organic dyes from wastewater is crucial to prevent environmental contamination and safeguard the public health.⁴

Recently, various methods and technologies have been proposed and utilized for treating wastewater contaminated with dyes. These methods include membrane filtration,⁵ biological treatment,⁶ oxidation, photocatalytic degradation,⁷ adsorption⁸ and coagulation-flocculation.⁹ Researchers widely use the adsorption method as an alternative for dye wastewater treatment.¹⁰ However, the efficiency of this process can be limited by the use of expensive adsorbents.¹¹

One of the most effective techniques for improving the adsorption process is to use various mineral or cement additives. These additives can be of natural origin, such as natural pozzolan, or artificial, such as lime or cement. They can also be mineral waste, such as silica fume, fly ash and so on. These materials exhibit distinct physicochemical and mineralogical characteristics.¹² Furthermore, low-cost materials, such as natural adsorbents, agricultural waste and by-products, have been proven effective in removing dyes.¹³ Clay minerals are considered as alternative materials to achieve this goal. According to many studies, bentonite clay can improve their properties in several fields.¹⁴ Bentonites are clay minerals, formed mainly by smectitic minerals in the form of lamellar silicates. In these minerals, their small particle size, less than 4 μm ,¹⁵ creates a large specific surface area and the presence of charge on the surfaces gives them unique physicochemical properties that allow them to attract substances from aqueous solutions. They are therefore widely used, among other important applications, to adsorb toxic compounds from aqueous media.¹⁶

However, it is a simple fact that clays have a low affinity for negatively charged anionic dyes. It is important to note that the adsorption capacities of clays can be significantly enhanced through a simple modification process using cationic polymers or surfactants. This can be achieved through straightforward ion-exchange reactions that create interactions between the cationic species and the adsorbate.¹⁷ Previous research has shown that using modified montmorillonite instead of raw montmorillonite greatly increases the effectiveness of acid dye removal.¹⁸ It is important to note that the synthesis of modified montmorillonites has already been reported and successfully used for the adsorption of Congo red dye.¹⁹ The study showed that the adsorption efficiency was significantly affected

by the length of alkyl chains in a series of alkyl ammonium bromides. Several authors have successfully modified montmorillonite using unconventional agents,²⁰ including gemini surfactants, to improve the adsorption of organic contaminants.²¹

This paper outlines a new approach for the modification of bentonite with starch and glycerol. The prepared composites were used as adsorbents to remove cationic (methylene blue) and anionic (methyl red) dyes. Various experimental parameters were examined to optimize the adsorption conditions. To assess the adsorption process, some kinetic studies were carried out.

EXPERIMENTAL

Materials

The material used in this study is the natural clay of Maghnia (Algeria), which is supplied by the ENOF company of bentonites.

One portion of the clay was used in the experiments, while the other was used for composite preparation. The procedure given for the preparation of the Bt@star@gly composite consists of mixing 5 g (5 %) bentonite in 45 mL of distilled water and then adding 0.75 g (30 %) glycerol and 0.125 g (5 %) starch to the suspension. On the other hand, the second composite (Bt@star) was prepared by the mixing of equal amounts by weight of bentonite and starch. The mixtures were then refluxed at a temperature of 80 °C for 4 h. After evaporating the water under reduced pressure, the resulting composites were manually ground and purified by stirring for 2 hours in distilled water to remove unreacted starting materials. Finally, the purified bio-composites were dried in an electric oven at 60 °C for 24 h.

The synthesized composites were evaluated for their mineralogical and structural properties using X-ray diffraction (XRD) with CuK α radiation ($\lambda = 1.54 \text{ \AA}$) at 40 kV and 30 mA, on a Rigaku Mini Flex 600. Fourier-transform infrared spectroscopy (FTIR) studies were conducted using the Agilent Cary 600 Series FTIR. The transmission spectra were obtained in the range of 4000–400 cm⁻¹.

Adsorption experiments

The batch equilibrium experiments were conducted to evaluate the adsorption capacities of the prepared composites for methylene blue (MB) and methyl red (MR). In each experiment, 25 mg of the composites were added to 25 ml of dye solutions with initial dye concentrations of 100 mg L⁻¹. The experiments were carried out in beakers with constant stirring at 400 rpm. The pH of the solution was adjusted within the range of 3 to 9 by the addition of drops of 1 M HCl or NaOH solutions. The contact time ranged from 5 to 120 min, while the initial dye concentration ranged from 100 to 500 mg L⁻¹. After adsorption, the adsorbent was separated from the liquid phase by centrifugation at 3000 rpm for 10 min. The supernatant was analysed using an Optizen 1412 UV/Vis spectrophotometer.

The adsorption capacity and removal efficiency were calculated from the initial and final concentrations of the dyes in the solution using the following equations:

$$q_e = (C_o - C_e)V/m \quad (1)$$

$$RE (\%) = 100(C_o - C_e)/C_o \quad (2)$$

where C_o and C_e denote the initial and equilibrium concentrations (mg L⁻¹) of the dye aqueous solution, V represents the volume of the dye solution (L) and m represents the mass (g) of the adsorbent used in each experiment.

RESULTS AND DISCUSSION

Adsorbents characterizations

Raw bentonite, Bt, Bt@star and Bt@star@gly adsorbent materials were characterized using XRD and FTIR techniques. The XRD diffractogram of raw bentonite, shown in Fig. 1a, indicates the presence of different diffraction peaks at 2θ 5.84, 15.7, 19.96, 21.0, 26.8, 35.1, 42.6, 46.0, 50.3, 54.8, 62.2, 68.3 and 73.3° , corresponding to different phases such as montmorillonite, quartz, calcite and magnesite.

These peaks were also observed in the biocomposites Bt@star and Bt@star@gly, with a single characteristic peak at 2θ $5\text{--}6^\circ$ indicating the basal spacing (d -spacing) of the silicate layers. The d -spacing for Bt was measured at 2θ 5.62° , with a value of 15.71 \AA . The d -spacing for Bt@star was slightly shifted to a higher angle, 2θ 5.97° , with a value of 14.77 \AA . This shift in the d -spacing suggests that the presence of starch polymer constricted the interlayer galleries of bentonite. It should also be noted that the chains of the polymer are mainly located on the outer surface of the bentonite clay. Angkawijaya *et al.* reported similar behaviour when modifying bentonite with chitosan.²²

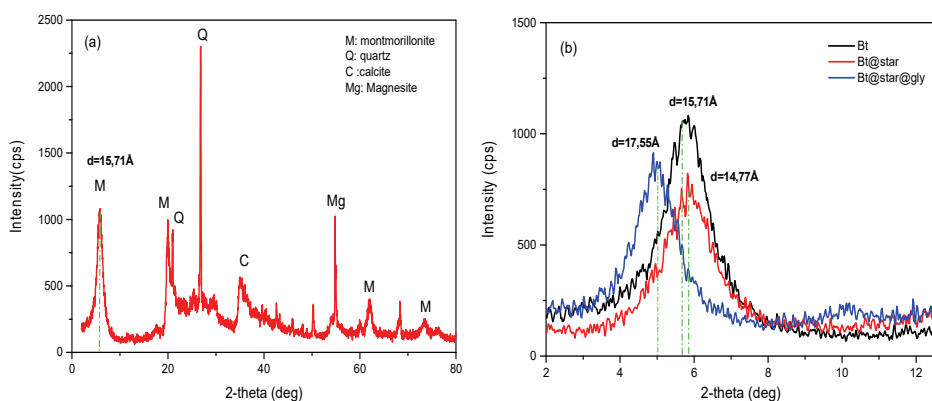


Fig. 1. XRD patterns of raw Bt (a); comparative d -basal spacing of Bt, Bt@star and Bt@star@gly (b).

Furthermore, as shown in Fig. 1b, the d -spacing for Bt@star@gly shifted to a lower angle of 2θ 5.03° with a value of 17.55 \AA . This increase in the d -spacing value confirms the success of the modification and the presence of glycerol in the basal space. These findings are consistent with results obtained using other molecules and macromolecules to modify bentonite, such as hexadecyltrimethylammonium bromide, cationic surfactant cetyltrimethyl ammonium bromide, graphene oxide, gelatine and poly(*N*-vinylpyrrolidone).^{18,23–26}

The XRD results are also in agreement with FTIR analysis. Fig. 2 displays the characteristic bands of corn starch, raw bentonite Bt and the biocomposites Bt@Star and Bt@Star@glyc.

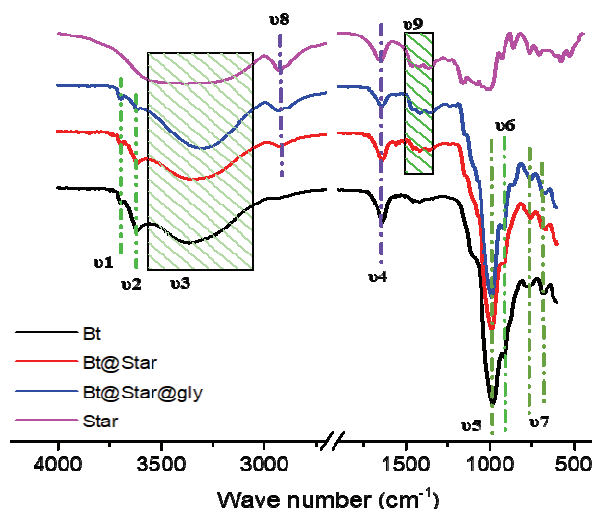


Fig. 2. FTIR spectra of the adsorbent materials.

The bands (v1 and v2) of raw bentonite at 3625 and 3701 cm^{-1} are caused by the vibrations of the OH groups of the water molecules adsorbed on the surface of the sample Bt. A broad absorption envelope (v3) was observed in the range from 3537 to 2987 cm^{-1} , which is attributed to the OH^- vibration of physically adsorbed water. Additionally, the bending mode of water was observed at 1635 cm^{-1} (v4).²⁷ The IR spectrum of Bt indicates the presence of the intense band (v5) centered at 981.51 cm^{-1} , which is related to the stretching vibration of the Si–O bonds. The 922 cm^{-1} (v6) band reveals the presence of amorphous SiO_2 .²⁸ Moreover, the bands at 688 and 775 cm^{-1} (v7) are attributed to the Al–O–Si–O bond and silanol group, respectively.

The FTIR spectra of Bt@Star and Bt@Star@glyc unquestionably exhibited a profile similar to that of raw bentonite. In addition, the spectra confirm the successful modification with the emergence of new bands at 2930 (v8) and around 1400 cm^{-1} (v9). These bands are attributed to the stretching vibration of the C–H bonds and the symmetric deformation of CH_2 groups and asymmetric stretching of C–H bonds.²⁹ The Bt@Star spectrum and the Bt@Star@glyc spectrum are clearly distinguishable. The two bands in question are more prominent in the Bt@Star@glyc composite. This is due to the presence of similar absorption bands in the glycerol spectra.³⁰ This observation unequivocally confirms the fixation of glycerol in the bentonite lattice, as previously demonstrated by XRD.

Methylene blue and methyl red dyes removal

Effect of pH. Numerous studies have shown that pH is a critical parameter in the adsorption process, as it affects both the functional groups of the adsorbent and the adsorbate. Therefore, this study investigated the removal of MB and MR dyes by native starch (Star), raw bentonite (Bt) and the composites Bt@Star and Bt@Star@glyc at three different pH values: 3, 6 and 9, using HCl (1 mol L⁻¹) and NaOH (1 mol L⁻¹). The results are presented in Fig. 3.

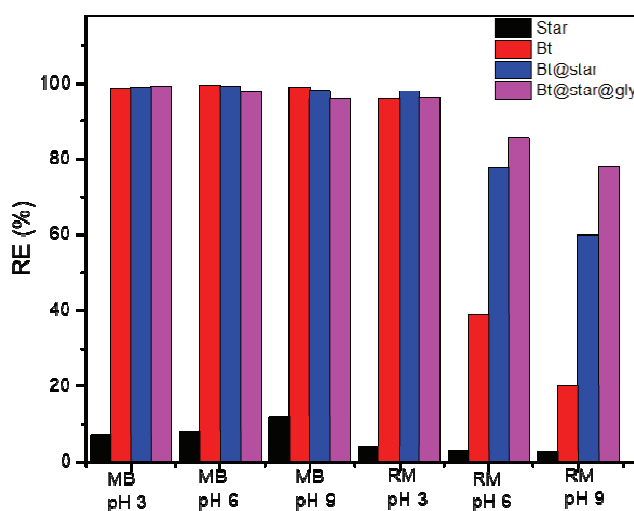


Fig. 3. MB and MR adsorption efficiency RE at different pH for Star, Bt, Bt@star and Bt@star@gly. [MB] = 100 mg L⁻¹, [MR] = 100 mg L⁻¹, V_{MB} and V_{MR} = 25 mL, m_{ads} = 25 mg, t = 60 min, T = 20 °C, 400 rpm.

Upon comparing the four adsorbents, the experimental data clearly show that the native corn starch has the lowest retention capacity, making it unsuitable for MB and MR retention.

The results for MB dye clearly show that Bt, Bt@star and Bt@Star@gly have a significant and similar retention capacity (*RE*) at both pH 3 and 6 (Fig. 3). At pH 3, the *RE* is 98.53, 98.99 and 99.19 % for Bt, Bt@star and Bt@Star@gly, respectively. At pH 6, the *RE* is 99.46, 99.23 and 97.53 % for Bt, Bt@star and Bt@Star@gly, respectively.

The retention efficiency is also very significant for the MR dye at pH 6. The value increased when starch and glycerol modifiers were added to the raw bentonite. The values were 95.95 % for Bt, 97.73 % for Bt@star and 96.19 % for Bt@Star@gly. The results clearly show that the addition of starch and glycerol has no negative effect on the adsorption capacity of the bentonite portion for the dyes.

The result for MR at pH 6 is undoubtedly the most important for the part in question. Fig. 3 clearly shows a significant increase in RE from 38.74 % for Bt to 77.71 % for Bt@Star and 85.58 % for Bt@Star@gly. This result definitively confirms the crucial role of modifying Bt with starch and glycerol, which creates a structure that interacts more effectively with cationic (MB) and anionic (MR) dyes.

In contrast, it is clear that the retention efficiency of MR dye consistently decreases for all adsorbent materials as the pH varies from 3 to 6 and then to 9. This can be mainly explained by the partial deprotonation of the adsorbent surface, which gives rise to a negative charge that prevents the interaction with MR molecules that already carry a negative charge specific to their carboxylate groups.³¹

Effect of contact time

Fig. 4a and b show the effect of contact time on the adsorption capacity of MB and MR dyes. In these experiments, 25 mg of each adsorbent was added to 25 ml of the dye's solutions with a concentration of 100 mg L^{-1} .

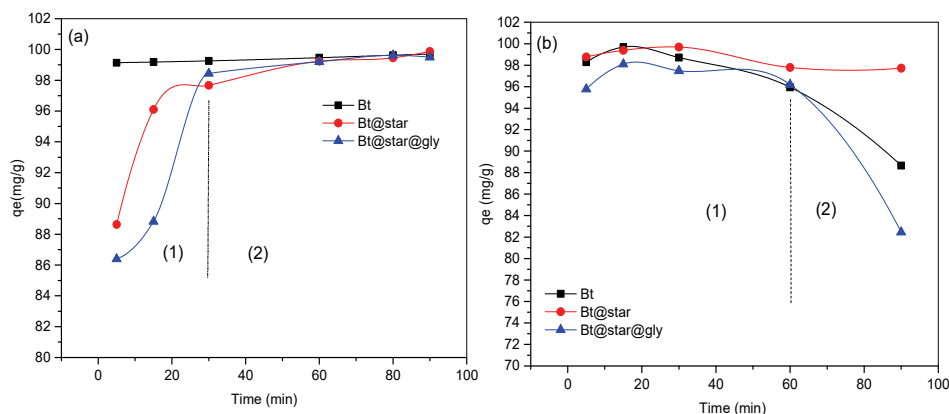


Fig. 4. Time-dependent q_e (mg g^{-1}) of MB (a) and MR (b) removed by Bt, Bt@star and Bt@star@gly. $[\text{MB}] = 100 \text{ mg L}^{-1}$, $[\text{MR}] = 100 \text{ mg L}^{-1}$, V_{MB} and $V_{\text{MR}} = 25 \text{ mL}$, $m_{\text{ads}} = 25 \text{ mg}$, $\text{pH } 6$, $T = 20 \text{ }^\circ\text{C}$, 400 rpm .

As shown in Fig. 4a, the adsorption of MB on the adsorbents Bt, Bt@star and Bt@star@gly is a fast process which can be divided into two distinct phases for the two composites. The first phase lasts for 30 min. During this time, the majority of the MB molecules are fixed on the surface of the adsorbents, then diffuse into the pores and the basal space of the biocomposites at a significant adsorption rate. In the second phase, the saturation of the active sites of the adsorbents resulted in a significant reduction in adsorption rate, with only a few molecules being adsorbed.

After 80 min of contact between the adsorbent and the adsorbate (second phase), the adsorption of MB reached a plateau, indicating that equilibrium had been reached. The presence of the plateau proves that the adsorption of MB has reached equilibrium under the considered experimental conditions and also proves that the adsorption rate is balanced by the desorption rate.

Fig. 4b clearly shows that the adsorption of MR on the used adsorbent materials is rapid. Fig. 4 also demonstrates that the retention of MR is highly efficient, with a q_e value of more than 95 mg g^{-1} in only 5 min of contact time. Fig. 4b also shows a contrasting reverse behaviour to that of Fig. 4a, with minimal fluctuation in retention capacity from 5 to 60 min (Part 1), then a gradual desorption of the adsorbed MR molecules on Bt@star and Bt@star@Gly (Part 2).

The experimental data were fitted with pseudo-first-order and pseudo-second-order models using Eqs. (3) and (4):

$$\text{Pseudo-first-order equation: } \log(q_e - q_t) = \log q_e - \frac{K_1}{2.303} t \quad (3)$$

$$\text{Pseudo-second-order equation: } \frac{t}{q_t} = \frac{1}{K_2 q_e^2} + \frac{1}{q_e} t \quad (4)$$

where K_1 (min^{-1}) is the pseudo-first order adsorption rate constant, K_2 ($\text{g mg}^{-1} \text{ min}^{-1}$) is the pseudo-second order adsorption rate constant and q_e (mg g^{-1}) is the adsorption capacity at equilibrium. These constants were determined from the slopes and intercepts of the lines obtained by plotting t/q_t versus t .

The graphical representations of this model are represented in Fig. 5 and the kinetic parameters obtained from the fitting are given in Table I. The comparison between calculated adsorption capacities $q_{e,\text{cal}}$ and experimental $q_{e,\text{exp}}$ values for each dye clearly suggests that the pseudo second order model describes the adsorption of MB and MR better. Similar results were reported by Mohammedi *et al.*^{32–34}

In addition, the correlation coefficients (R^2) confirm that the adsorption of MB and MR on each adsorbent studied is described by the pseudo-second order model, indicating a multistage adsorption process. The adsorption rate is therefore dependent on the number of active sites in the adsorbent material. These results are consistent with the previous studies, which also found that the adsorption of methylene blue and methyl red on various materials follows the pseudo-second order model.^{35–37}

Effect of MB and MR dose on the adsorption performance and isotherm study. The effect of initial dye concentration was investigated in the range of 100 to 500 mg L^{-1} . Fig. 6a–c show that the amount of dye retained by each adsorbent increases with increasing initial dye concentration. For an initial concentration of MB equal to 500 mg L^{-1} , the adsorption capacity achieved was 203.78 mg g^{-1}

($RE = 40.75\%$), 146.21 mg g^{-1} ($RE = 29.24\%$) and 157.58 mg g^{-1} ($RE = 31.51\%$) for Bt, Bt@star and Bt@star@gly, respectively. The MR dye q_e values are substantial, proving that the three materials are excellent adsorbents for removing both anionic and cationic dyes. The obtained adsorption capacities are equal to 309.81 mg g^{-1} ($RE = 61.96\%$), 426.38 mg g^{-1} ($RE = 85.27\%$) and 309.82 mg g^{-1} ($RE = 61.96\%$) for Bt, Bt@star and Bt@star@gly, respectively. To compare, the Table II clearly shows that the composites used in this study have better adsorption capacities (q_{\max}) than many other materials reported so far in the literature.^{29,38–45}

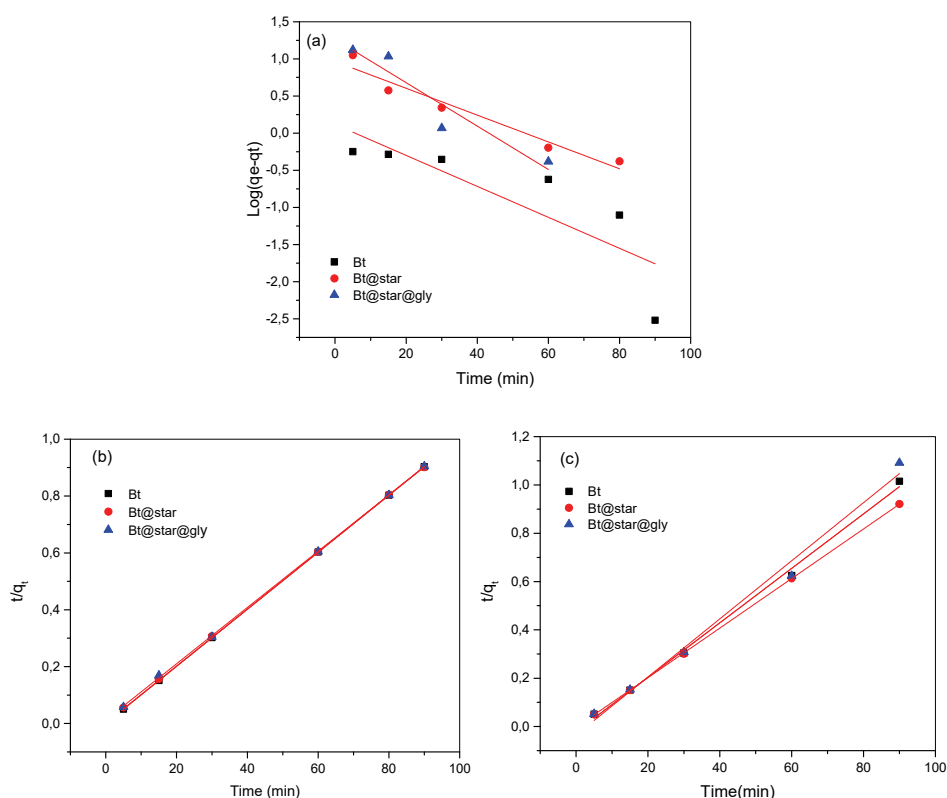


Fig. 5. Linear fit by using the pseudo-first order model of the retention of MB (a) and the linear fit by using pseudo-second order model for the retention of MB (b) and MR (c).

TABLE I. Characteristic parameters obtained by pseudo-first order; pseudo-second order

Dye	Material	$q_{e,exp}$ mg g^{-1}	1 st order			2 nd order		
			K_1 / min^{-1}	$q_{e,cal} / \text{mg g}^{-1}$	R^2	$K_2 / \text{mg g}^{-1} \text{min}^{-1}$	$q_{e,cal} / \text{mg g}^{-1}$	R^2
MB	Bt	99.69	0.0479	1.31	0.703	0.1137	99.70	1
	Bt@star	99.69	0.0415	9.22	0.950	0.0134	100.50	0.999
	Bt@star@gly	99.87	0.067	18.34	0.904	$8.06 \cdot 10^{-3}$	101.01	0.9998

TABLE I. Continued

Dye	Material	$q_{e,exp}$ mg g ⁻¹	1 st order			2 nd order		
			K_1 / min^{-1}	$q_{e,cal} / \text{mg g}^{-1}$	R^2	$K_2 / \text{mg g}^{-1} \text{min}^{-1}$	$q_{e,cal} / \text{mg g}^{-1}$	R^2
MR	Bt	99.69	Not applicable			0.0113	88.65	0,9961
	Bt@star	99.61	Not applicable			0.0103	97.46	0,9999
	Bt@star@gly	98.09	Not applicable			0.0119	83.33	0,9901

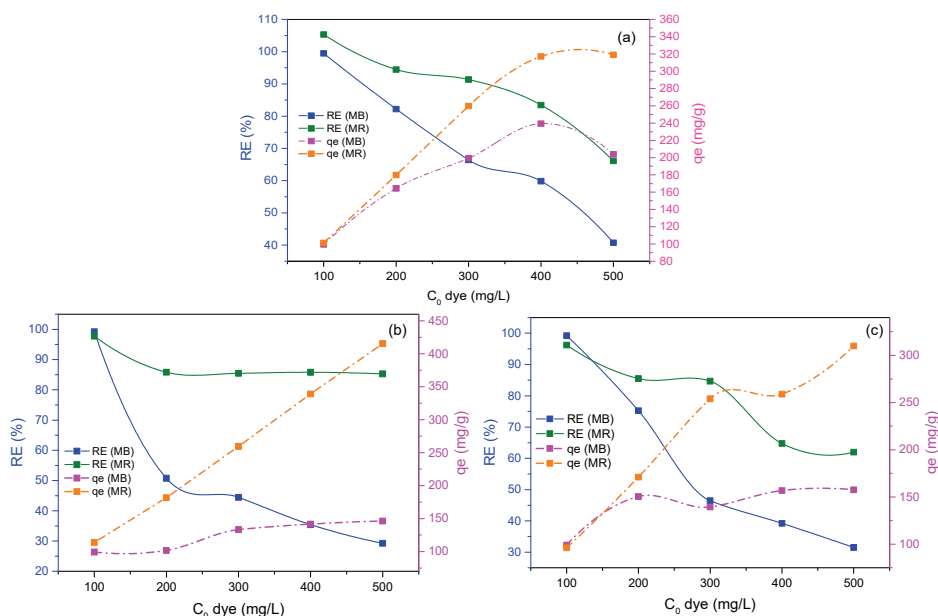


Fig. 6. MB and MR removal capacity (q_e) and removal efficiency (RE) as a function of the initial dye concentration by using: a) Bt, b) Bt@star and c) Bt@star@gly. V_{MB} and $V_{MR} = 25$ mL, $m_{ads} = 25$ mg, pH 6, $T = 20$ °C, 400 rpm, $t = 60$ min.

In order to obtain information about the adsorption isotherms, the experimental data were fitted to the Langmuir and Freundlich adsorption models using Eqs. (5) and (6), respectively. The curves obtained are shown in Figs. 7a–d:

$$\text{Langmuir equation: } \frac{C_e}{q_e} = \frac{1}{K_1 Q_{max}} + \frac{C_e}{Q_{max}} \quad (5)$$

$$\text{Freundlich equation: } \log q_e = \log K_F + \frac{1}{n} \log C_e \quad (6)$$

where K_1 is the Langmuir constant (L mg^{-1}), Q_{max} is the maximum adsorption capacity (mg g^{-1}), C_e the concentration at equilibrium (mg L^{-1}), K_F the Freundlich constant (mg g^{-1}) and n is the adsorption intensity.

Table III shows the values obtained for the constant parameters of the Langmuir and Freundlich adsorption isotherms. The correlation coefficient values clearly

TABLE II. Maximal adsorption capacity q_{\max} for MB and MR removal by different materials

Dye	Material	$q_{\max} / \text{mg g}^{-1}$	Reference
MB	Hydroxyapatite@starch composite	45.51	29
	Calcined hydroxyapatite	38.93	37
	Biogas plant waste	147	38
	Starch biocryogel	34.84	39
	Diatomite	66.7	40
	Montmorillonite modified tea waste biochar	27.89	41
	Bt	203.78	This work
	Bt@star	146.21	
	Bt@star@gly	157.58	
	MR	Biogas plant waste	115
Bark of Hopbush		36.64	42
Orange peel		111.11	43
Carbon clay/alginate membrane		248.14	44
Anionic surfactant		53.59	45
Bt		309.81	This work
Bt@star		426.38	
	Bt@star@gly	309.82	

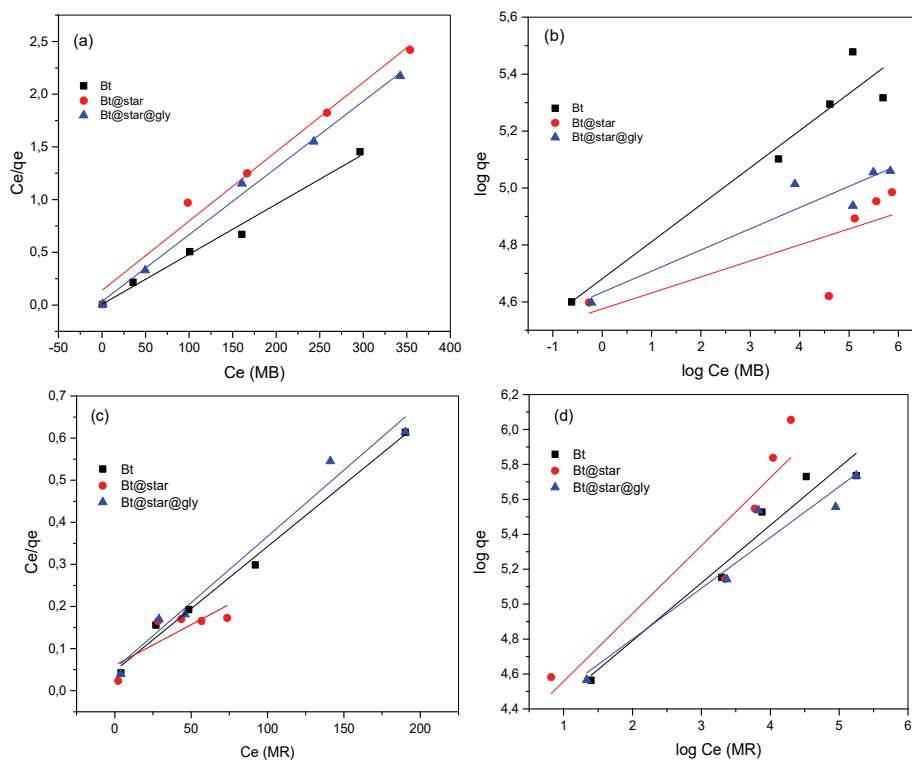


Fig. 7. Linear fits of the experimental data of MB (a, b) and MR (c, d) by using Langmuir and Freundlich isotherm models, respectively.

indicate that the adsorption of MB and MR dyes onto Bt and Bt@star@gly is better described by the Langmuir model. The applicability of the Langmuir model suggests that the adsorbent surface is homogeneous, resulting in the monolayer adsorption. This unequivocally demonstrates that all the binding sites present in Bt and Bt@star@gly are energetically equivalent.

TABLE III. Isotherm parameters for MB and MR adsorption by Bt, Bt@star and Bt@star@gly samples according to Langmuir and Freundlich models

Material	Dye	Freundlich			Langmuir		
		n	K_F	R^2	$q_{\max} / \text{mg g}^{-1}$	K_L	R^2
Bt	MB	7.6863	107.8994	0.909	210.97	0.661	0.986
	MR	3.0257	62.1592	0.938	338.98	0.063	0.989
Bt@star	MB	17.7935	97.0474	0.441	151.98	0.051	0.978
	MR	2.5753	64.6831	0.827	518.13	0.032	0.543
Bt@star@gly	MB	13.4408	102.8734	0.874	157.98	0.184	0.994
	MR	3.4376	67.8771	0.913	317.46	0.061	0.973

The Langmuir model also describes the adsorption of MB by the composite material Bt@Star. Nevertheless, the Freundlich isotherm model is the best fit for the adsorption of MR, indicating the existence of multilayer adsorption. This explains the important adsorption capacity of 426.38 mg g^{-1} at an initial MR concentration of 500 mg L^{-1} .

CONCLUSION

The present investigation showed the significant results regarding the adsorption of methylene blue and methyl red using bentonite and its composites. The described modification significantly improves the adsorptive capacity of bentonite, making these composites highly effective adsorbents for anionic dyes. Furthermore, the study proves that using readily available natural materials is the most effective way to minimize both starting material costs and experimental expenses. The application of adsorption on modified bentonite is undoubtedly a promising approach for the removal of pollutants from water.

ИЗВОД

ПОБОЉШАНА СВОЈСТВА АДОРПЦИЈЕ АЛЖИРСКОГ БЕНТОНИТА МОДИФИКОВАНОГ СКРОБОМ И ГЛИЦЕРОЛОМ ЗА ЗАДРЖАВАЊЕ МЕТИЛЕНСКОГ ПЛАВОГ И МЕТИЛ-ЦРВЕНОГ

FATIMA ZAHRA BENHACHEM^{1,2}, HANANE MAHROUG^{2,3}, MERIEM BENDJELLOUL⁴, ABDELKADER MIRAOU^{1,2},
EL HADJ ELANDALOUSSI⁴, KHALIL OUKEBDANE² И RANIA HALFAOUI⁵

¹Department of Industrial Engineering, Faculty of Technology, University of Tlemcen, Tlemcen, Algeria,

²Laboratory of Separation and Purification Technologies, Department of Chemistry, Faculty of Sciences, University of Tlemcen, Tlemcen, Algeria, ³Department of Hydraulic, Institute of Sciences and Technology, University center of Maghnia, Algeria, ⁴Environment and Sustainable Development Laboratory, Department of Chemistry, Faculty of Sciences u Technology, University of Relizane, Algeria u ⁵Department of Chemistry, Faculty of Sciences, University of Tlemcen, Tlemcen, Algeria

У раду је описана припрема нових композита бентонит–скроб и оцењена је њихова ефикасност као адсорбенса за уклањање боја метиленског плавог (МВ) и метил-црвеног

(MR) из водених раствора. Адсорбенси су окарактерисани коришћењем рендгенске дифракције и FTIR спектроскопије. Студија је имала за циљ да оптимизује процес уклањања боја испитивањем утицаја рН, дозе адсорбенса, времена контакта и почетне концентрације. Кинетика сорпције МВ и MR боје је анализирана коришћењем модела псеудо-првог и псеудо-другог реда. Експериментални резултати показују да кинетички модел псеудо-другог реда најбоље одговара. Композитни адсорбенси су показали сорпциони капацитет за МВ у распону од 146,21 до 157,58 mg g⁻¹ за бентонит–скроб (Bt@star) и бентонит–скроб–глицерол (Bt@star@gly), редом. Капацитет сорпције за MR боју био је 426,38 mg g⁻¹ за Bt@star и 309,82 mg g⁻¹ за Bt@star@gly. Штавише, вредности коефицијента корелације показују да се адсорпција МВ и MR од стране Bt@star@gly најбоље описује Ленгмировим моделом. Ово недвосмислено имплицира да је површина адсорбенса хомогена, што резултира једнослојном адсорпцијом. Ленгмир модел такође тачно описује адсорпцију МВ на Bt@star. Међутим, Фројндлихов модел изотерме је најбољи за адсорпцију MR, што указује на постојање вишеслојне адсорпције. Коначно, ова студија показује да композитни адсорбенти који су овде припремљени показују одличне резултате адсорпције и могу бити исплатива алтернатива за третман обојене отпадне воде.

(Примљено 29. фебруара, ревидирано 22. априла, прихваћено 24. новембра 2024)

REFERENCES

1. K. Nagaraja, M. Arunpandian, T. H. Oh, *J. Polym. Environ.* **32** (2024) 4538 (<https://doi.org/10.1007/s10924-024-03225-5>)
2. A. A. Adesibikan, S. S. Emmanuel, C. O. Olawoyin, P. Ndungu, *J. Org. Chem.* **1010** (2024) 123087 (<https://doi.org/10.1016/j.jorganchem.2024.123087>)
3. S. Dutta, S. Adhikary, S. Bhattacharya, D. Roy, S. Chatterjee, A. Chakraborty, D. Banerjee, A. Ganguly, S. Nanda, P. Rajak, *J. Environ. Manage.* **353** (2024) 120103 (<https://doi.org/10.1016/j.jenvman.2024.120103>)
4. M. B. Etsuyankpa, A. U. Augustine, S. T. Musa, J. T. Mathew, H. Ismail, A. M. Salihu, A. Mamman, *J. Appl. Sci. Environ. Manage.* **28** (2024) 5 (<https://doi.org/10.4314/jasem.v28i5.28>)
5. R. J. Kadhim, F. H. Al-Ani, Muayad Al-shaeli, Q. F. Alsahy, A. Figoli, *Membranes* **10** (2020) 366 (<https://doi.org/10.3390/membranes10120366>)
6. I. A. Saleh, N. Zouari, & M. A. Al-Ghouti, *Environ. Technol. Innov.* **19** (2020) 2352 (<https://doi.org/10.1016/j.eti.2020.101026>)
7. I. Mahboob, I. Shafiq, S. Shafique, P. Akhter, M. Munir, M. Saeed, M. S. Nazir, U.-e-S. Amjad, F. Jamil, N. Ahmad, Y.-K. Park, M. Hussain, *Chemosphere* **311** (2023) 137180 (<https://doi.org/10.1016/j.chemosphere.2022.137180>)
8. F. Z. Benhachem, M. Bendjelloul, H. Mahroug, A. Miraoui, E.H. Elandaloussi, K. Oukebdane, R. Halfaoui, *J. Dispers. Sci. Technol.* (2024) (<https://doi.org/10.1080/01932691.2024.2378193>)
9. L. Sablii, O. Obodovych, V. Sydorenko, *J. Serb. Chem. Soc.* **90** (2025) 247 (<https://doi.org/10.2298/JSC231206014S>)
10. A. Miraoui, L. Mitiche, F.Z. Benhachem, S. Feddane, M. Bendjelloul, E.H. Elandaloussi, M.A. Didi, *Iran. J. Chem. Chem. Eng.* **43** (2024) 3989 (<https://doi.org/10.30492/ijcce.2024.2025988.6527>)
11. S. Lin, Z. Song, G. Che, A. Ren, P. Li, C. Liu, J. Zhang, *Microporous Mesoporous Mater.* **193** (2014) 27 (<https://doi.org/10.1016/j.micromeso.2014.03.004>)

12. H. Gadouri, K. Harichane, M. Ghrici, *Per. Poly. Civ. Eng.* **61** (2017) 256 (<https://doi.org/10.3311/PPci.9359>)
13. S. Mishra, L. Cheng, A. Maiti, *J. Environ. Chem. Eng.* **9** (2021) 104901 (<https://doi.org/10.1016/j.jece.2020.104901>)
14. R. Marouf, N. Dali, N. Boudouara, F. Ouadjenia, F. Zahaf, in *Montmorillonite Clay*. F. Uddin, Ed., *IntechOpen*, Rijeka, 2021 (<https://doi.org/10.5772/intechopen.96524>)
15. F. Bergaya, G. Lagaly, *Dev. Clay Sci.* **1** (2006) 1 ([https://doi.org/10.1016/S1572-4352\(05\)01001-9](https://doi.org/10.1016/S1572-4352(05)01001-9))
16. R. Zhu, Q. Chen, Q. Zhou, Y. Xi, J. Zhu, H. He, *Appl. Clay Sci.* **123** (2016) 239 (<https://doi.org/10.1016/j.clay.2015.12.024>)
17. E. M. Ö. Kaya, A. S. Özcan, Ö. Gök, A. Özcan, *Adsorption* **19** (2013) 879 (<https://doi.org/10.1007/s10450-013-9542-3>)
18. Z. Baouch, K.I. Benabadji, B. Bouras, *Phys. Chem. Res.* **8** (2020) 767 (<https://doi.org/10.22036/pcr.2020.234691.1787>)
19. L. Wang, A. Wang, *J. Hazard. Mater.* **160** (2008) 173 (<https://doi.org/10.1016/j.jhazmat.2008.02.104>)
20. Ö. Açışlı, S. Karaca, A. Gürses, *Appl. Clay Sci.* **142** (2017) 90 (<https://doi.org/10.1016/j.clay.2016.12.009>)
21. S. Yang, M. Gao, Z. Luo, *Chem. Eng. J.* **256** (2014) 39 (<https://doi.org/10.1016/j.cej.2014.07.004>)
22. A. E. Angkawijaya, S. P. Santoso, V. Bundjaja, F. E. Soetaredjo, C. Gunarto, A. Ayucitra, Y. Ju, A.W. Go, S. Ismadji, *J. Hazard. Mater.* **399** (2020) 123130 (<https://doi.org/10.1016/j.jhazmat.2020.123130>)
23. P. Huang, A. Kazlauciušas, R. Menzel, L. Lin, *ACS Appl. Mater. Int.* **31** (2017) 26383 (<https://doi.org/10.1021/acsami.7b08406>)
24. Z. Taibi, K. Bentaleb, Z. Bouberka, C. Pierlot, M. Vandewalle, C. Volkringer, P. Supiot, U. Maschke, *Crystals* **13** (2023) 211 (<https://doi.org/10.3390/cryst13020211>)
25. S. Merad Boudia, K. I. Benabadji, B. Bouras, *Phys. Chem. Res.* **33** (2022) 143 (<https://doi.org/10.22036/pcr.2021.290926.1925>)
26. D. Heddi, A. Benkhaled, A. Boussaid, E. Chekchou Braham, *Phys. Chem. Res.* **7** (2019) 731 (<https://doi.org/10.22036/pcr.2019.179510.1625>)
27. K. Atkovska, B. Bliznakovska, G. Ruseska, S. Bogoevski, B. Boskovski, A. Grozdanov, *J. Chem. Technol. Metall.* **51** (2016) 215
28. B. Makhoukhi, M. Djab, M. A. Didi, *J. Environ. Chem. Eng.* **3** (2015) 1384 (<https://doi.org/10.1016/j.jece.2014.12.012>)
29. H. Mahroug, S. Belkaid, *Phys. Chem. Res.* **12** (2023) 73 (<https://doi.org/10.22036/pcr.2023.374016.2244>)
30. M. R. Nanda, Z. Yuan, W. Qin, M. A. Poirier, X. Chunbao, *Austin J. Chem. Eng.* **1** (2014) 1004 (<https://austinpublishinggroup.com/chemical-engineering/fulltext/ace-v1-id1004.php>)
31. S. Rangabhashiyam, N. Anu, N. Selvaraju, *J. Environ. Chem. Eng.* **1** (2013) 629 (<https://doi.org/10.1016/j.jece.2013.07.014>)
32. S. Z. Mohammadi, N. Mofidinasab, M.A. Karimi, A. Beheshti, *Int. J. Environ. Sci. Technol.* **17** (2020) 4815 (<https://doi.org/10.1007/s13762-020-02767-0>)
33. S. Z. Mohammadi, Z. Safari, N. Madady, *Appl. Surf. Sci.* **514** (2020) 145873 (<https://doi.org/10.1016/j.apsusc.2020.145873>)
34. S. Z. Mohammadi, N. Mofidinasab, M. A. Karimi, F. Mosazadeh, *Water. Sci. Technol.* **82** (2020) 829 (<https://doi.org/10.2166/wst.2020.375>)

35. M. El-Habacha, A. Dabagh, S. Lagdali, Y. Miyah, G. Mahmoudy, F. Sinan, M. Chiban, S. Laich, M. Zerbet, *Environ. Sci. Pollut. Res.* (2023) (<https://doi.org/10.1007/s11356-023-27413-3>)
36. Y. A. B. Neolaka, Y. Lawa, J. Naat, A. C. Lalang, B. A. Widyaningrum, G. F. Ngasu, K. A. Niga, H. Darmokoesoemo, M. Iqbal, H. S. Kusuma, *Results Eng.* **17** (2023) 100824 (<https://doi.org/10.1016/j.rineng.2022.100824>)
37. M. Aaddouz, K. Azzaoui, N. Akartasse, E. Mejdoubi, B. Hammouti, M. Taleb, R. Sabbahi, S. F. Alshahateet, *J. Mol. Struct.* **1288** (2023) 135807 (<https://doi.org/10.1016/j.molstruc.2023.135807>)
38. R. Wolski, A. Bazan-Wozniak, R. Pietrzak, *Molecules* **28** (2023) 6712 (<https://doi.org/10.3390/molecules28186712>)
39. T. Taweekarn, W. Wongniramaikul, C. Boonkanon, C. Phanrit, W. Sriprom, W. Limsakul, W. Towanlong, C. Phawachalotorn, A. Choodum, *Polymers* **14** (2022) 5543 (<https://doi.org/10.3390/polym14245543>)
40. N. A. Fathy, S. M. Mousa, R.M. Aboelenin, M.A. Sherief, A. S. Abdelmoaty, *Arab. J. Geosci.* **15** (2022) 1664 (<https://doi.org/10.1007/s12517-022-10891-z>)
41. R. Liu, Y. C. Li, Z. Zhao, D. Liu, J. Ren, Y. Luo, *Front. Environ. Sci.* **11** (2023) 1137284 (<https://doi.org/10.3389/fenvs.2023.1137284>)
42. S. Gul, M. Kanwal, R. A. Qazi, H. Gul, R. Khattak, M. S. Khan, F. Khitab, A. E. Krauklis, *Water* **14** (2022) 2831 (<https://doi.org/10.3390/w14182831>)
43. S. Deshmukh, N. S. Topare, S. Raut-Jadhav, P. V. Thorat, S. A. Bokil, A. Khan, *Aqua Water. Infrastruct. Ecosyst. Soc.* **71** (2022) 1351 (<https://doi.org/10.2166/aqua.2022.119>)
44. N. Ullah, Z. Ali, A. Sada Khan, B. Adalat, A. Nasrullah, S. Bahadar Khan, *RSC Adv.* **14** (2024) 211 (<https://doi.org/10.1039/D3RA07554K>)
45. Y. N. Teixeira, J. M. C. Menezes, R. N. P. Teixeira, F. J. Paula Filho, T. M. B. F. Oliveira, *Textiles* **3** (2023) 52 (<https://doi.org/10.3390/textiles301000>).